Practical Realization of Implicit Homogeneous Controllers for Linearized Systems

David Cruz-Ortiz, Mariana Ballesteros, Andrey Polyakov, Denis Efimov, Isaac Chairez, Alexander Poznyak

HAL Id: hal-03253670

https://inria.hal.science/hal-03253670

Submitted on 8 Jun 2021

Practical Realization of Implicit Homogeneous Controllers for Linearized Systems

David Cruz-Ortiz, Mariana Ballesteros, Andrey Polyakov,
Denis Efimov, *Senior Member*, Isaac Chairez and Alexander Poznyak

Abstract—This paper deals with the practical implementation of implicit homogeneous controllers (IHCs) for linearized mechanical systems. The control design includes the methodology to get gains of the IHC based on the linearized approximation of the system. If the approximation error enforced by the linearization is vanishing with the state, locally measurable and bounded, the IHC can lead the state to the origin in finite-time. This IHC control allows accelerating the convergence rate of the states. A semi-explicit algorithm is provided to exert the digital implementation of the controller. The application of the bisection method estimates the controller gain ensuring the finite-time convergence of the state to the origin. A complementary analysis provides a simplified algorithm with a reduced number of computation stages but equally efficient gain estimation. The proposed IHC is applied to a rotary inverted pendulum QUBE™ Servo 2 platform of Quanser®. The obtained results for the state convergence are compared with other classical feedback controllers to validate the effectiveness of the proposed scheme. The comparative analysis of the state convergence provides evidence of the faster convergence for the state trajectory to a zone centered on the origin with a smaller hypervolume than the one gotten with the classical controllers.

Index Terms—Nonlinear Control, Implicit Homogeneous Control, Inverted pendulum

I. Introduction

NUMEROUS control techniques (model-based and model-free) have been developed to solve the set-point stabilization problem for mechanical systems. Some of these techniques provide practical stabilization in a compact set centered at the equilibrium point. For example, state feedback controllers (usually known as Proportional-Derivative) and Linear Quadratic Regulators have been designed using the linearization around an equilibrium point, yielding the characterization of attractive invariant sets for the system trajectories. On the other hand, nonlinear schemes, such as robust approaches [1], sliding mode control (SMC) [2], among others, also have been implemented. Theoretically, all the previous controllers ensure asymptotic convergence of the state to the equilibrium point, without the presence of perturbations or measurement noises. However, due to several reasons (like measurement errors, non-modeled dynamics, and external perturbations) just a practical stabilization (convergence to an invariant and attractive set centered on the origin) can be guaranteed for real systems. Due to its simplicity, high efficiency and robustness, SMC (see [3]) is one of the most popular control methodologies to solve the stabilization problem of mechanical systems. Despite its relevant advantages, chattering (unexpected high-frequency oscillations) is a well-known drawback of SMC, implying severe degradation of the regulation quality in practice. High order SMC (see e.g. [4]) is a possible solution to the chattering problem. However, these controllers still may have chattering, and their gains design is still a matter of researching (see [5], [6], [7] and [8]). The application of homogeneity theory can serve to generalize the SMC designs and to remove some of their recognized drawbacks [9].

In addition, inconsistent digital realizations of homogeneous controllers (such as SMC) can be a relevant reason for the chattering presence (see [10], [11] and [12]) (the so-called *numerical chattering*) and some other undesired behaviors in the performance of mechanical systems. Therefore, a proper discretization (digital implementation) is required for its successful further practical application. Consequently, it is necessary to provide the justified methodology (including the selection of the gains) to solve the discretization issues with the homogeneous control practical implementation on real plants. Implicit Lyapunov theory was proposed as a reliable method to get efficient gains (state-dependent) estimations of homogeneous controllers [7]. However, these designs still suffer from the implementation aspects, including the design of the proper discretization technique.

In the last few years, some advanced discretization methods have appeared to solve the implementation of homogeneous controllers. Despite the efficient realization of such discretized controllers, there is still a necessity to provide simplified methodologies to design the gains of the implemented controllers that may ensure the consistent realization of homogeneous controllers, in particular those calculated using the implicit Lyapunov technique.

This manuscript describes an implicit homogeneous con-

D. Cruz-Ortiz is with the Automatic Control Department, CINVESTAV-IPN, 2508 Av. IPN, 07360 Mexico City, and with UPIBI - Instituto Politécnico Nacional, 550 Av. Acueducto, 07340 Mexico City, Mexico. (e-mail: dcruzo@ipn.mx.)

M. Ballesteros and **I. Chairez** are with UPIBI - Instituto Politécnico Nacional, 550 Av. Acueducto, 07340 Mexico City, Mexico, and with Tecnologico de Monterrey, School of Engineering and Sciences, Guadalajara, Mexico. (e-mail: mballesterose, ichairezo@ipn.mx.)

A. Polyakov and **D. Efimov** are with Inria, Univ. Lille, CNRS, UMR 9189 - CRIStAL, F-59000 Lille, France and Department of Control Systems and Informatics, University ITMO, 49 Av. Kronverkskiy, 197101 Saint Petersburg, Russia. (e-mail: andrey.polyakov, denis.efimov@inria.fr)

A. Poznyak is with the Automatic Control Department, CINVESTAV-IPN, 2508 Av. IPN, 07360 Mexico City, Mexico. (e-mail: apoznyak@ctrl.cinvestav.mx)

trol (IHC) (see [7], [9] and [13]) to regulate the linearized approximation of nonlinear mechanical systems. The control design is essentially based on the so-called canonical homogeneous norm [9], which defines an implicit Lyapunov function that leads to the obtention of the control gains design [14], [15]. Moreover, the corresponding methodology to achieve a successful implementation on a real plant is presented. In this study, the inverted pendulum (IP) was considered to verify the suggested implementation method of the implicit Lyapunov based controller. The IP is a nonlinear system with multiple equilibrium points. This robotic system is similar to some devices used in diverse industrial and academic applications, such as biped robots [16], segways [17] and monocycles [18]. This device was selected considering that it is one of the most popular options to test the effectiveness of different robust control schemes [19]. For example, the study in [20] presents a novel adaptive neural network-based control scheme to solve the trajectory tracking problem of an IP. The article proposed by [21] developed a novel high-order disturbance observer for the Mobile Wheeled IP system. Also, different estimation algorithms have been tested for the IP device [22]. The QUBE™ Servo 2 system developed by Quanser® is used as an IP experimental setup to evidence the effectiveness of the proposed controller. The IHC proposed in this study is applied considering the preliminary application of a suitable swing-up controller [23].

The **main contributions** of the current manuscript are:
- The proposed control design applies to a class of perturbed linear systems (more general form than the required in [7]). That means, the class of linear systems considered can be easily obtained as a result of the application of classic linearization methods over nonlinear plants (real plants) or considering linear dominant nonlinear systems.
- The proper transformation to drive a linear system in the companion controllable form to the required form in [7] is provided in a constructive approach, that is, step by step.
- From a practical implementation point of view, numerous real plants have been stabilized using a linear feedback controller that in most cases has been optimized for these particular plants. Then, since the proposed controller can start from a previously designed linear controller, the implementation of the proposed methodology improves the performances obtained without the necessity of a complicated methodology design. All the implementation steps are specified in the paper, including the proper linear transformation (Remark 3), the controller gain design by solving a LMI (Section III-A) aside from the algorithm to implement the bisection method, which is the main tool to compute the proposed controller gain.
- The implementation of the proposed controller has been tested on an actual Furuta pendulum. Then, it might be easy for readers to create analogies with the objective to implement the proposed controller in more complex actual plants.

Paper organization: In the following sub-section, some useful definitions are presented. Section II describes the problem statement. In section III, the IHC and its inverse design from an existing LC are presented. Section IV discusses the semi-explicit discretization scheme for the digital implementation of the IHC. Section V describes the experimental setup.

Finally, Section VI closes the study with some conclusions.

A. Preliminaries

In this part of the manuscript, some important definitions for the IHC design and its implementation on a mechanical device are described.

1) Homogeneous Systems: Homogeneity is a certain symmetry of functions (operators, sets, vector fields, etc.) with respect to a group of transformations known as dilations. The group of linear **dilations** (see [9], [24]), $x \to \mathbf{d}(s)x$, $x \in \mathbb{R}^n$, $s \in \mathbb{R}$, is defined as $\mathbf{d}(s) = e^{G_{\mathbf{d}}s}$, where $s \in \mathbb{R}$ is a group parameter. The matrix $G_{\mathbf{d}} \in \mathbb{R}^{n \times n}$ is known as **generator** of the dilation, $-G_{\mathbf{d}}$ is a Hurwitz matrix. Notice that if $G_{\mathbf{d}} = I_n$, then $\mathbf{d}(s)$ defines the standard (uniform) dilation $x \to \lambda x$ with $\lambda = e^s$. The dilation group $\mathbf{d}(s)$ is said to be **strictly monotone** if there exists $\beta > 0$, such that $\|\mathbf{d}(s)\| \le e^{\beta s}$ for $s < 0$.

Lemma 1. *Let the norm $\|\cdot\|_P$ in $\mathbb{R}^n$ be defined as follows $\|x\|_P = \sqrt{x^\top P x}$, $0 < P = P^\top \in \mathbb{R}^{n \times n}$. Then, the dilation $\mathbf{d}(s)$ is strictly monotone if and only if $G_{\mathbf{d}}^\top P + P G_{\mathbf{d}} > 0$ [9].*

For monotone dilations, the **canonical homogeneous norm** $\|\cdot\|_{\mathbf{d}}$ can be induced by an original (canonical) norm, $\|\cdot\|$ (Euclidean norm) or $\|\cdot\|_P$ in $\mathbb{R}^n$ as $\|x\|_{\mathbf{d}} = e^{s_0}$, $s_0 : \|\mathbf{d}(-s_0)x\| = 1$. The parameter s_0 defines the so-called homogeneous projection of the vector x to the unit sphere.

Lemma 2. *The canonical homogeneous norm $\|\cdot\|_{\mathbf{d}} : \mathbb{R}^n \to [0, +\infty)$ is a continuous, single-valued and positive definite function $\|\mathbf{d}(s)x\|_{\mathbf{d}} = e^s \|x\|_{\mathbf{d}}$, $\forall x \in \mathbb{R}^n$, $\forall s \in \mathbb{R}$. Moreover, it is continuously differentiable on $\mathbb{R}^n \setminus \{0\}$, provided that the original norm $\|\cdot\|$ is also continuously differentiable on $\mathbb{R}^n \setminus \{0\}$ [24].*

2) Implicit Homogeneous Controller: The next result is a straightforward corollary of Theorem 1 from [24] (see also [9] and [13] for more details about its application in finite-dimensional cases).

Corollary 1. *Let $A_0 \in \mathbb{R}^{n \times n}$ be **d**-homogeneous matrix of degree $\nu < 0$, i.e.*

$$A_0 G_{\mathbf{d}} - G_{\mathbf{d}} A_0 = \nu A_0. \tag{1}$$

Let $B_0 \in \mathbb{R}^{n \times m}$ satisfy the identity $G_{\mathbf{d}} B_0 = -\nu B_0$, and the pair $\{A_0, B_0\}$ be controllable in the Kalman sense [25]. If there exist $K \in \mathbb{R}^{m \times n}$, $P \in \mathbb{R}^{n \times n}$ and $\alpha \in (0, +\infty)$, such that

$$\begin{aligned} (A_0 + B_0 K)^\top P + P(A_0 + B_0 K) + \alpha(G_{\mathbf{d}}^\top P + P G_{\mathbf{d}}) \le 0, \\ G_{\mathbf{d}}^\top P + P G_{\mathbf{d}} > 0, \quad P > 0, \end{aligned} \tag{2}$$

then, the control $u = K\mathbf{d}(-\ln \|x\|_{\mathbf{d}})x$, $x \in \mathbb{R}^n$, where the canonical homogeneous norm $\|x\|_{\mathbf{d}}$ is induced by the weighted Euclidean norm $\|x\|_P$, stabilizes the state of the system $\dot{x} = A_0 x + B_0 u$, $x(0) = x_0$, to the equilibrium point in a finite-time, i.e. there exists $T(x_0) \le \frac{1}{\alpha}\|x_0\|_{\mathbf{d}}$, such that $x(t) \to 0$ as $t \to T(x_0)$.

The parameter α can be used for tuning the finite-time convergence. Notice that the control u is **d**-homogeneous of degree 0, i.e. $u(\mathbf{d}(s)x) = u(x)$, $\forall x \in \mathbb{R}^n$, $\forall s \in \mathbb{R}$. Below, we show how to apply this result for stabilization of linearized mechanical systems. Since the homogeneous norm $\|\cdot\|_{\mathbf{d}}$ is

defined implicitly, the obtained control law can be called IHC.

II. PROBLEM STATEMENT

The class of nonlinear systems considered in this manuscript is governed by

$$\dot{x} = A_m x + f(x) + g(x)u, \quad A_m = \begin{bmatrix} 0_{n/2} & I_{n/2} \\ 0_{n/2} & 0_{n/2} \end{bmatrix}, \quad (3)$$

where $x \in \mathbb{R}^n$ is the state vector (n an even integer), $u \in \mathbb{R}^m$ is the control input, the vector field $f : \mathbb{R}^n \to \mathbb{R}^n$ and the matrix associated to the input $g : \mathbb{R}^n \to \mathbb{R}^{n \times m}$ define the system dynamics [26].

The **main goals** of the paper are to develop a control law such that the origin of the closed-loop system (3) is a stable equilibrium point in a finite-time and to provide a methodology to get a proper discretization of the IHC (digital implementation), including the sequential steps to achieve successful implementation in a real plant.

The control algorithm should have an effective scheme for tuning the control parameters. Therefore, a novel methodology named inverse design of the IHC is presented. The inverse design approach allows the estimation of the corresponding control gains from an existing LC, which may result in a simplified design.

Remark 1. *The control design (IHC extension) proposed in this study and its implementation methodology can be applied to feedback linearizable nonlinear multi-input multi-output systems (See [7]).*

In most applications, the model of the real mechanical plant has some model uncertainties, or the process is affected by bounded perturbations. In addition, for design issues, it is usual to consider the system is formed by a nominal known section and the remainder (uncertain section) that satisfy some assumptions, such as uniform boundedness, Lipschitz condition, among others, depending on the considered control design. Homogeneous approximations for control plants as (3) are also usually used for design issues. For homogeneous representations, if the autonomous nonlinear system can be represented as the sum of two homogeneous structures (with different degrees of homogeneity), the stability analysis can be globally conclusive considering the stability of the part with the smallest homogeneity degree [27], [28]. In addition, if it is not possible to represent the nonlinear system with homogeneous structures only, it is feasible to obtain local practical stability for the origin in a compact set [29].

Taking into consideration the dynamics of (3), a feasible representation to implement the IHC considers the Taylor expansion around the equilibrium point of the nonlinear system, that is

$$\dot{x} = Ax + bu(x) + h(x), \quad A \in \mathbb{R}^{n \times n}, b \in \mathbb{R}^n. \quad (4)$$

The high order terms (beyond the first-order approximation) are denoted by $h : \mathbb{R}^n \to \mathbb{R}^n$. The aforementioned representation can be understood as the simplest case of the homogeneous representation for linearized systems. Notice that mechanical systems are quite susceptible to admit the linearized representation considering the significant number of control approaches that have exploited the local linear

dominant behavior of such class of nonlinear systems [30]. For autonomous nonlinear systems, the study of the linear approximation section could give a conclusion about the stability in a compact set around the linearization point (equilibrium point), and the stability analysis in closed-loop of the system can be conclusive considering the degree of homogeneity, such as finite-time convergence and robustness, at least in the compact. Therefore, if h satisfies the condition $\|h(x)\|/\|x\| \to 0$ as $\|x\| \to 0$, it is still possible to argue that the origin is a local robust stable equilibrium point implementing the homogeneous controller [7], and its convergence is in finite-time. Moreover, if the function h is measurable locally bounded uniformly in time, such that: $\sup_{x \in \mathbb{R}^n : \|x\| < \Psi} \|h(x)\| < \infty$ for any $\Psi > 0$, the result of the stability can be extended globally [7].

For the considered class of systems in this work, the remaining aspects included in the implementation of the IHC can also be considered uniformly bounded if the control design may provide a zero homogeneity degree for the closed-loop system.

III. IMPLICIT HOMOGENEOUS CONTROL DESIGN

Intending to design a proper method to construct the IHC, this study uses a particular example based on a classical mechanical system, the IP, which is a two degree of freedom robotic device.

A. Experimental Setup: Inverted Pendulum

In Figure 1, a schematic representation of the rotary IP is depicted. The generalized coordinates θ and δ describe the angular positions of the rotary arm and the pendulum, respectively. To obtain the motion equations, the pendulum is considered as a lumped mass at its geometric center.
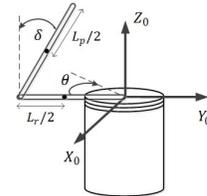

Fig. 1. Schematic diagram of inverted pendulum (IP)

The following variables describe the parameters of the IP model considered in this work, the mass of the pendulum (m_p), length of the pendulum (L_p), pendulum inertia (J_p), pendulum damping coefficient (D_p), Length of the rotary arm (L_r), rotary arm inertia (J_r), viscous damping coefficient (D_r) and gravitational acceleration (g_p). The dynamic model is derived by means of the Euler-Lagrange method [31]. The variable $q \in \mathbb{R}^2$ represents the vector of the generalized coordinates, given by $q := \begin{bmatrix} \theta, & \delta \end{bmatrix}^\top$. Therefore, the dynamic model is described by:

$$J(q)\ddot{q} + C(q,\dot{q})\dot{q} + w(q) = \phi, \quad (5)$$

where, $w(q) = [0, -0.5g_p m_p L_p \sin(\delta)]^\top$, $\phi = [\tau, 0]^\top$,

$$J(q) = \begin{bmatrix} J_r + \psi + \frac{1}{4}(\zeta - \zeta \cos^2(\delta)) & -\frac{1}{2}\varpi \cos(\delta), \\ -\frac{1}{2}\varpi \cos(\delta) & J_p + \frac{1}{4}\zeta \end{bmatrix},$$

$$C(q) = \begin{bmatrix} \frac{1}{2}\zeta \sin(\delta)\cos(\delta)\dot{\delta} + D_r & \frac{1}{2}\varpi \sin(\delta)\dot{\delta} \\ -\frac{1}{4}\zeta \sin(\delta)\cos(\delta)\dot{\theta} & D_p \end{bmatrix},$$

with $\zeta = m_p L_p^2$, $\psi = m_p L_r^2$ and $\varpi = m_p L_p L_r$. The torque generated by the servo motor and applied to the rotary arm is described by $\tau = R_m^{-1} k_m (V_m - k_m \dot{\theta})$, where k_m is the electromotive force constant, R_m is the terminal resistance and V_m is the control input, in other words, it is the input voltage for the servo motor.

Remark 2. *Notice that the dynamic model used in this manuscript matches the dynamic model described by the experimental setup manufacturer. Moreover, all the assumptions considered to obtain the linearized model and in consequence the values obtained for A and b match with the considerations and values reported by Quanser®. The previous fact could be verified in [32]. The intention to use the parameter values given by Quanser® is to evidence the improvement offered by the IHC compared with the manufacturer LC.*

B. Local approximation

Notice that (5) can be represented according to the expression given in (4) by choosing the state variables $x_1 = \theta$, $x_2 = \delta$, $x_3 = \dot{\theta}$ and $x_4 = \dot{\delta}$. Therefore, the linearization outcome by taking the operating point $\delta = 0$ (upper position of the pendulum, following the Quanser® procedure), $\theta = 0$, $\dot{\delta} = 0$ and $\dot{\theta} = 0$, considering (5) for δ close to zero one gets $\sin(x_2) \approx 0$, $\cos(x_2) \approx 1$. Therefore, the linearized representation for the IP satisfies:

$$\dot{x}_1 = x_3, \quad \dot{x}_2 = x_4,$$
$$\dot{x}_3 = \frac{-(J_p + 0.25\zeta)D_r x_3 - 0.5\varpi D_p x_4 + 0.25\vartheta g x_2 + (J_p + 0.25\zeta)\tau}{J_T}, \quad (6)$$
$$\dot{x}_4 = \frac{0.5\varpi D_r x_3 - (J_r + \psi)D_p x_4 + 0.5 m_p L_p g(J_r + \psi)x_2 + 0.5\varpi\tau}{J_T},$$

where $J_T = J_p \zeta + J_r J_p + 0.25 J_r \zeta$ and $\vartheta = m_p^2 L_p^2 L_r$.

By considering the previous dynamic system, the control design presented below considers $n = 4$ to evidence its implementation on a real IP. Therefore, after some algebraic manipulations, the previous equation admits the linearized state-space representation for the IP given in (4) where $x = [x_1, x_2, x_3, x_4]^\top \in R^4$ is the state vector, $u \in R$ is the control input, $A \in R^{4\times4}$, $b \in R^4$ are the system matrices with the following elements:

$$A = \begin{bmatrix} 1 & 0 & 0 & 0 \\ 0 & 1 & 0 & 0 \\ 0 & 0 & J_T^{-1} & 0 \\ 0 & 0 & 0 & J_T^{-1} \end{bmatrix} \begin{bmatrix} 0 & 0 & 1 & 0 \\ 0 & 0 & 0 & 1 \\ 0 & a_{3,2} & a_{3,3} & a_{3,4} \\ 0 & a_{4,2} & a_{4,3} & a_{4,4} \end{bmatrix}, b = \begin{bmatrix} 1 & 0 & 0 & 0 \\ 0 & 1 & 0 & 0 \\ 0 & 0 & J_T^{-1} & 0 \\ 0 & 0 & 0 & J_T^{-1} \end{bmatrix} \begin{bmatrix} 0 \\ 0 \\ J_p + 0.25\zeta \\ 0.5\varpi \end{bmatrix}, \quad (7)$$

where $a_{3,2} = 0.25\vartheta g_p$, $a_{3,3} = -(J_p + 0.25\zeta)D_r$, $a_{3,4} = -0.25\varpi D_p$, $a_{4,2} = 0.25 m_p L_p g_p(J_r + \psi)$, $a_{4,3} = 0.25\varpi D_r$, and $a_{4,4} = -(J_r + \psi)D_p$.

Let consider (4) for the selected mechanical system, with matrix $A \in R^{4\times4}$ and vector $b \in R^4$, satisfying that the pair $\{A, b\}$ is controllable in the Kalman sense [25], and consider $\phi_A = \lambda^4 + \alpha_1 \lambda^3 + \alpha_2 \lambda^2 + \alpha_3 \lambda$ be the characteristic polynomial of the matrix A, and the following coordinate transformation $z = \Phi x$, $\Phi := [e_1, e_2, e_3, e_4]^{-1}$ with $e_1 = A^3 b + \alpha_1 A^2 b + \alpha_2 A b + \alpha_3 b$, $e_2 = A^2 b + \alpha_1 A b + \alpha_2 b$, $e_3 = A b + \alpha_1 b$ and $e_4 = b$. Since the pair $\{A, b\}$ is controllable, then the transformation Φ is non-singular and the next Lemma can be proven.

Lemma 3. *The matrix $A_0 \in R^{4\times4}$, defined by $A_0 = A - b[0, 0, 0, 1]\Phi A$, is **d**-homogeneous of degree*

$-\mu$, *with respect to the dilation group* $\mathbf{d}(s) = e^{G_{\mathbf{d}}s}$, $G_{\mathbf{d}} = \Phi^{-1} diag\{4\mu, 3\mu, 2\mu, \mu\}\Phi$, *and* $G_{\mathbf{d}}b = \mu b$, *where* $\mu \in (0, 1]$.

Proof. A set of calculations justifies $G_{\mathbf{d}}b = \Phi^{-1}diag\{4\mu, 3\mu, 2\mu, \mu\}\Phi b$, where $b = [0, 0, 0, 1]^\top$, then the previous equation can be rewritten as follows $G_{\mathbf{d}}b = \Phi^{-1}diag\{4\mu, 3\mu, 2\mu, \mu\}[0, 0, 0, 1]^\top$. Therefore, $G_{\mathbf{d}}b = \mu\Phi^{-1}[0, 0, 0, 1]^\top$. That is equal to $G_{\mathbf{d}}b = \mu b$. Considering that

$$\Phi A_0 \Phi^{-1} = \tilde{A} := \begin{bmatrix} 0 & 1 & 0 & 0 \\ 0 & 0 & 1 & 0 \\ 0 & 0 & 0 & 1 \\ 0 & 0 & 0 & 0 \end{bmatrix}.$$

Hence, we derive $\Phi(A_0 G_{\mathbf{d}} - G_{\mathbf{d}}A_0)\Phi^{-1} = -\mu\tilde{A}$, that can be expressed as $\Phi(A_0 G_{\mathbf{d}} - G_{\mathbf{d}}A_0)\Phi^{-1} = -\mu\Phi A_0\Phi^{-1}$, i.e. the identity (1) holds. $\square$

Therefore, all conditions of Corollary 1 are fulfilled and the control

$$u(x) = \left(ke^{-G_{\mathbf{d}} \ln \|x\|_{\mathbf{d}}} - [0, 0, 0, 1]\Phi A \right) x \quad (8)$$

stabilizes all trajectories of (4) to the origin in finite-time, providing that $k = yX^{-1} \in R^{1\times4}$ is given by

$$A_0 X + X A_0^\top + B_0 y + y^\top B_0^\top + \alpha(G_{\mathbf{d}}X + XG_{\mathbf{d}}) \leq 0, \quad (9)$$
$$X G_{\mathbf{d}} + G_{\mathbf{d}}X > 0, \quad 0 < X \in R^{4\times4},$$

where $B_0 = \Phi b$, the canonical homogeneous norm $\|x\|_{\mathbf{d}}$ is induced by $\|x\|_P$, with $P = X^{-1}$, and $\alpha > 0$ is a constant parameter to adjust the settling time of the closed-loop system. Notice that for any $x \in R^4$ the system of matrix inequalities (9) has a solution with respect to (X, y) [33].

C. On Inverse Design of IHC

The gain matrix k of the control law (8) can be found using the gain matrix $k_{lin} \in R^{1\times4}$ of some already designed LC. Indeed, it is sufficient to assume that the LC $k_{lin}x$ and the homogeneous one (8) coincide on the unit sphere $\|x\|_{\mathbf{d}} = 1$. Hence, we immediately derive

$$k = k_{lin} + [0, 0, 0, 1]\Phi A. \quad (10)$$

In order to find a matrix P required for calculation of the canonical homogeneous norm $\|x\|_{\mathbf{d}}$ induced by $\|x\|_P$, the following system of linear matrix inequalities (LMI) needs to be solved

$$(A_0 + B_0 k)^\top P + P(A_0 + B_0 k) + \alpha(PG_{\mathbf{d}} + G_{\mathbf{d}}P) \leq 0, \quad (11)$$
$$PG_{\mathbf{d}} + G_{\mathbf{d}}P > 0, \quad P > 0,$$

where α, $G_{\mathbf{d}}$, A, A_0 and B_0 are already defined.

Remark 3. *Notice that if the external perturbations acting over the IP has to be considered in an explicit form on the control design, the linearized model can be transformed as* $\dot{x} = Ax + bu(x) + h(x) + \xi(t)$, $A \in R^{4\times4}$, $b \in R^4$, *where* $\xi : R \to R^4$ *describes the internal uncertainties and external bounded perturbations affecting the mechanical system. The term ξ satisfies $\|\xi\| \leq \xi^+ < \infty$, $\forall t \geq 0$. Therefore, to get global stability conclusions based on the homogeneity of the proposed controller we need the inclusion of the bounds for the high order elements in the linearized representation (4) of (3), as well as the upper bound of the externals perturbations (ξ^+). In other words, a slight change in inequality (2) of Corollary 1, including the bounds for the high order terms provides the*

claimed global result. The new matrix inequality that must be solved is formulated in [7]. For the particular case considered in this study, such matrix inequality corresponds to:

$$(A_0 + B_0 K)^\top P + P(A_0 + B_0 K) + \alpha(G_\mathbf{d}^\top P + PG_\mathbf{d}) + \bar{\Psi} I_4 \leq 0,$$
$$G_\mathbf{d}^\top P + PG_\mathbf{d} > 0, \quad P > 0,$$

where I_4 represents the identity matrix with dimension 4×4 and $\bar{\Psi} = \Psi + \xi^+$.

Notice that the main novelty of this work is to introduce a constructive framework for the digital implementation of the IHC and the called inverse design to improve a classical linear feedback controller. The practical realization of the state-dependent gain for the IHC represents a contribution to the control engineering practice.

IV. IHC IMPLEMENTATION METHODOLOGY

Figure 2 shows the block diagram detailing how the proposed design and implementation scheme for the homogeneous control can be realized for the IP platform QUBE™, Servo 2. The implementation uses the application developed by the Quanser® company to exert the real-time interaction between the implemented controller and the experimental platform. By considering the block diagram given in Figure
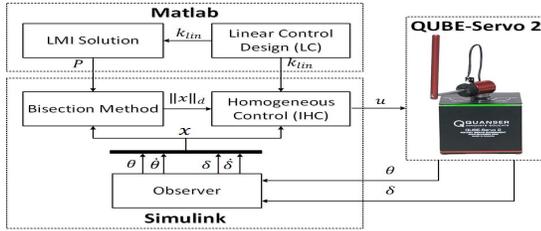

Fig. 2. QUBE™ Servo 2 in closed-loop with the IHC.

2, the steps to implement the IHC in the IP system can be summarized as follows.

1.- Consider the nonlinear model of the real plant.

2.- Compute the linearized model of the real plant to obtain the matrix A and vector b.

3.- Under the assumption that the pair $\{A, b\}$ is controllable, the matrix transformation Φ given in Section III B must be computed.

4.- By considering the matrix transformation Φ, the new matrix A_0 of the linear system can be computed by using the expression given in Lemma 3.

5.- The control gain matrix should be calculated by solving the matrix inequality given in (9).

6.- Finally, the control law given in (8) must be computed by using the bisection method provided in Algorithm 1. In addition, if the real plant that must be controlled has a previously designed LC, the following two additional steps can be implemented to improve the performance offered by the LC.

7.- Compute the new control gain matrix by using the expression given in (10).

8.- By using matrix inequality (11), compute the value of matrix P and then the control law given in (8) must be computed by using the bisection method provided in Algorithm 1.

Remark 4 (On the State Observer). *To apply the IHC, the full state x must be known online. However, the device allows the on-line measurement of the angles δ and θ only. The approach suggested by the manufacturer to obtain the velocity consists of the implementation of two high pass filters on the measured data of the position angles θ and δ. Based on the user manual [32], the high pass filter proposed by Quanser® is described by the following transfer function $T(s) = 50s/s + 50$. In the experimental setup, the velocities $\dot{\theta}$ and $\dot{\delta}$ are assumed to be estimated exactly as the manufacturer suggested. There are several ways to design differentiators to estimate the velocities (see e.g. [3] and [34]), however, the closed-loop analysis considering the estimates and the output feedback realization of IHC is not considered in this paper.*

A. Semi-explicit digital implementation

For the digital implementation, the matrix $P \in \mathbb{R}^{4\times4}$ and the gain matrix $k \in \mathbb{R}^{1\times4}$ in (8) are defined using the inverse IHC design, this is, (10) and (11) must be considered. To implement the control law (8), the value of $\|x\|_\mathbf{d}$ is needed, then, it is necessary to apply a method to compute it. Formally, the equation

$$\|\mathbf{d}(-\ln r)x\|_P = 1, \tag{12}$$

should be numerically on-line solved with respect to the scalar $r \in (0, +\infty)$, by the definition of the canonical homogeneous norm, we derive $r = \|x\|_\mathbf{d}$. For this purpose, we introduce Algorithm 1 based on the bisection method to get the aforementioned calculus (see [35], Chapter 2.1 The bisection algorithm). The algorithm should be implemented at each

---

Algorithm 1 Bisection Algorithm

Require: A current state $x \in \mathbb{R}^4$ of the system and the variables $0 < a < b < +\infty$ initialized as $a = a_{\min}$ and $b = b_{\max}$ at the initial instant of time.

Ensure: $\|x\|_\mathbf{d} \approx b$ (after several iterations)
1: **if** $\|\mathbf{d}(-\ln b)x\|_P > 1$ **then**
2:      $a = b$, $b = \min(2b, b_{\max})$
3: **else if** $\|\mathbf{d}(-\ln b)x\|_P < 1$ **then**
4:      $a = b$, $a = \max(a/2, a_{\min})$
5: **else**
6:      **for** $j = 1, ..., j_{\max}$ **do**
7:          $c = (a+b)/2$
8:          **if** $\|\mathbf{d}(-\ln c)x\|_P < 1$ **then**
9:              $b = c$
10:          **else**
11:              $a = c$
12: **return** a, b

---

sampling instant time to estimate $\|x\|_\mathbf{d}$. The sampling period is defined by the selected digital device used for control computation. The parameters a, b are assumed to be initialized in the first instant of time. The interval $[a, b]$ is used for the estimation of $\|x\|_\mathbf{d}$. Lines 1-6 of the algorithm are introduced to estimate the root of equation (12). Lemma 2 guarantees that it has a unique and positive real root for any $x \neq 0$. Lines 8-13 realize the bisection method, which operates only when $\|x\|_\mathbf{d} = r \in [a, b]$. The commands in the loop (lines 9-13) decrease the length of the interval $[a, b]$ two times thereby

improving the precision of the root estimation. Algorithm 1 has constant parameters which must be tuned for each concrete control plant:

- The constant positive matrix $0 < P = P^\top \in \mathbb{R}^{4 \times 4}$;
- The anti-Hurwitz constant matrix $G_{\mathbf{d}} \in \mathbb{R}^{4 \times 4}$ which defines a generator of dilation group $\mathbf{d}$ in $\mathbb{R}^4$
- Constant parameters $0 < a_{\min} \le b_{\max} < +\infty$ which restrict upper and lower values of $\|x\|_{\mathbf{d}}$ for practical implementation;
- The natural number $j_{\max}$ which defines the number of bisection iterations. The matrix $G_{\mathbf{d}}$ is defined by the model plant and the matrix P can be obtained from the system of matrix inequalities (11) which can be easily solved off-line (e.g. in Matlab®). The parameter $j_{\max}$ should be selected depending on the speed of the computational device. For a larger j_{max}, a more precise estimate of $\|x\|_{\mathbf{d}}$ can be derived. However, increasing the precision of the obtained root with the algorithm requires more computational cost. The value of $j_{\max}$ is an integer $j_{\max} \ge 1$. The parameters $a_{\min}$ and $b_{\max}$ as well as $j_{\max}$ need to be tuned manually for the concrete plant. *If we select $a_{\min} = b_{\max} = 1$ then the control scheme given in Figure 2 generates the LC $u = k_{lin}x$.* To observe this fact, it is enough to substitute $\|x\|_{\mathbf{d}}$ with 1 in (8), since Algorithm 1 always returns a not-null outcome as an approximation of the homogeneous norm. To improve the convergence rate, the parameter $a_{\min}$ needs to be decreased, as long as, this improves the control performance. Theoretically, for $a_{\min} = 0$ we should have a finite-time convergence. Therefore, the following algorithm for practical tuning of the parameters $a_{\min}$ and $b_{\max}$ is suggested: *Step 1*: selection of $a_{\min} = b_{\max} = 1$ (i.e. starting with a LC). *Step 2*: decrease $a_{\min}$ and increase (if necessary) $b_{\max}$ as long as this result on an improvement of the control performance.

Notice that if a LC is already optimally tuned, the performance is not largely improved. However, such approach does not imply performance degradation, because in the worst case, only the performance of the original LC is obtained.

Remark 5. *In order to minimize the number of computations in Algorithm 1, notice that the inequality $\|\mathbf{d}(-\ln b)x\|_P > 1$ is equivalent to $x^\top e^{-G_{\mathbf{d}}^\top \ln b} P e^{-G_{\mathbf{d}} \ln b} x > 1$. Moreover, one has*

$$e^{-G_{\mathbf{d}} \ln b} = e^{\Phi^{-1} diag\{4\mu,3\mu,2\mu,\mu\}\Phi \ln b^{-1}} = \Phi^{-1} e^{diag\{4,3,2,1\} \ln b^{-\mu}} \Phi$$

$$= \Phi^{-1} diag\{b^{-4\mu}, b^{-3\mu}, b^{-2\mu}, b^{-\mu}\}\Phi.$$

This result implies that the inequality $\|\mathbf{d}(-\ln b)x\|_P > 1$ is equivalent to

$$\left(b^{-4\mu} \ b^{-3\mu} \ b^{-2\mu} \ b^{-1\mu}\right) \tilde{P}(x) \left(b^{-4\mu} \ b^{-3\mu} \ b^{-2\mu} \ b^{-1\mu}\right)^\top > 1,$$

where $\tilde{P}(x) = \text{diag}\{z\}\Phi^{-\top}P\Phi^{-1}\text{diag}\{z\}$, $z = \Phi x$. Therefore, for $\mu = 1$, to check the condition $\|\mathbf{d}(-\ln b)x\|_P > 1$, we just need to compute powers of the scalar b^{-1} up to order four and the value of the quadratic form.

The proposed scheme to solve the implementation of the IHC (8) discretization is explicit. It does not use implicit Euler discretization as for example for prediction of the system state as in [11]. However, it still uses a solver for a nonlinear equation (similar to the implicit Euler scheme) to find $\|x\|_{\mathbf{d}}$. That is why this scheme is called *semi-explicit*. Below, we show the experiments with the rotary IP that the developed approach allows us to design the IHC which significantly improves the control performance of the original LC proposed

by the manufacturer. Notice that the proposed methodology can be easily implemented for other mechanical systems with a larger number of degrees of freedom. This study aims to offer a tutorial approach to the design and practical implementation of IHC. The next section exemplifies the application of the proposed methodology.

V. EXPERIMENTAL EVALUATION OF THE IHC ON REAL IP

In order to validate the control scheme suggested above, the real-time experimentation on the QUBE™ Servo 2 platform was performed. The parameters of the experimental platform are given by the manufacturer: $m_p = 0.024\ Kg$, $L_p = 0.129\ m$, $J_p = 3.3 \times 10^{-5}\ Kg.m^2$, $D_p = 0.0015\ N \cdot m \cdot s/rad$, $L_r = 0.085$ m, $J_r = 5.7 \times 10^{-5}\ Kg.m^2$, $D_r = 0.0005\ N \cdot m \cdot s/rad$, $g_p = 9.81$ m/s^2. Also, the nominal electrical and mechanical parameters values of the DC motor has been provided that is: nominal input voltage ($V_{nom} = 18\ V$), nominal current ($I_{nom} = 0.540$ A), nominal torque ($\tau_{nom} = 22\ mN \cdot m$), terminal resistance ($R_m = 8.4\ \Omega$), the electromotive force constant ($k_m = 0.042$ $V \cdot s/rad$) the rotor inertia ($J_m = 4.0 \times 10^{-6}\ Kg.m^2$) and the rotor inductance ($L_m = 1.16\ mH$), for more details see [32]. A controller stabilizing the IP in an upper position consists of two feedback laws. The first one is a swing-up controller, which by means of increasing the amplitude of input oscillations, brings the pendulum into a neighborhood of the upper (unstable) position. Then, (after ≈ 1.5 sec), a locally stabilizing controller is applied. This strategy is valid considering the attraction region of the equilibrium point corresponding to the upper vertical orientation of the LP. In the experiment, we compare only two locally stabilizing controllers: a LC and the IHC. The corresponding system matrices are

$$A = \begin{bmatrix} 0 & 0 & 1 & 0 \\ 0 & 0 & 0 & 1 \\ 0 & 149.2751 & -0.0104 & 0 \\ 0 & 261.6091 & -0.0103 & 0 \end{bmatrix}, \quad b = \begin{bmatrix} 0 \\ 0 \\ 49.7275 \\ 49.1493 \end{bmatrix}.$$

The feedback gain of the LC supported by the manufacturer is given by $k_{lin} = \begin{bmatrix} 2 & -30 & 2 & -2.5 \end{bmatrix}$. The gain matrix k of the IHC is obtained using (10), that is $k = \begin{bmatrix} -113.4482 & -108.1254 & -13.7505 & -0.2833 \end{bmatrix}$. The matrix P is obtained from (11) with $\mu = 1$ and $\alpha = 1 \times 10^{-3}$.

$$P = \begin{bmatrix} 0.1304 & 0.0053 & 0.0213 & 0.0844 \\ 0.0053 & 0.1729 & 0.0344 & 0.1168 \\ 0.0213 & 0.0344 & 0.3037 & 0.2127 \\ 0.0844 & 0.1168 & 0.2127 & 0.3930 \end{bmatrix}.$$

These parameters obeys the values previously stated (*Lemma 3* and (9), respectively) and were tuned manually in order to obtain a better performance, the value $\mu = 1$ results in a particular class of control (high order sliding mode). The parameter α regulates the settling time of the closed-loop system (See [7]) as the theoretical result confirms. Practical selection for the value of parameter α: For both cases, when the user have a previous LC or for the direct implementation of the IHC, the parameter can be chosen as follows, set the value equal to one, if the LMI solver provides a feasible solution for P, the velocity convergency will depend on the selected μ. For this study with $\mu = 1$ the converge correspond to a high order sliding mode control rejecting matched bounded disturbances, $0 < \mu < 1$ the controller ensures uniform finite-time stability, otherwise with $\mu = 0$ the controller ensures uniform asymptotically stability [7]. If setting $\alpha = 1$ the user

does not get a feasible solution with the solver, the value could be decreased until the solution for P is obtained. To realize the practical implementation, the parameters required for solving the Algorithm 1 are selected as follows $a_{\min} = 0.88$, $b_{\max} = 1$, $j_{max} = 3$. The experimental realization of the controller was resolved in the Simulink/Matlab application provided by Quasner with the integration method selected as the Runge-Kutta with a step of 0.0001 seconds.

Figure 3 shows the comparison between the stabilization results (angular positions) of the QUBE™ Servo 2 in closed-loop with an LC, SMC and the IHC. Notice that the implementation of the IHC produces similar transient trajectories for both angular displacements to the LC and SMC. However, IHC produces a smaller steady state error as predicted by the implementation methodology proposed in this study. Moreover, this controller exhibits oscillations with smaller amplitude that the LC, which is a remarkable outcome of the IHC. The interior figures show the trajectories endorsed by the IHC in the time range between 5 and 7 s. These steady states are closer to zero as predicted the theoretical results when the IHC is implemented, despite the discretization implementations. Both figures also show that once the trajectories are coming closer to the origin, the amplitude of oscillations are also reduced, which is a consequence of the homogeneity for the proposed controller. Figure 4 shows the time evolution of the
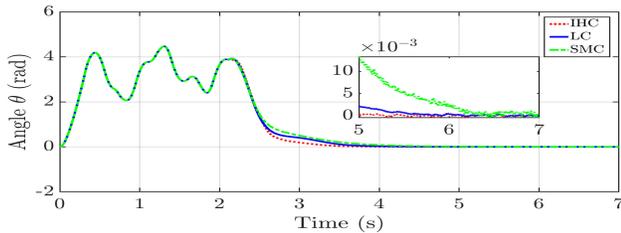
(a) Performance of rotary arm (θ)
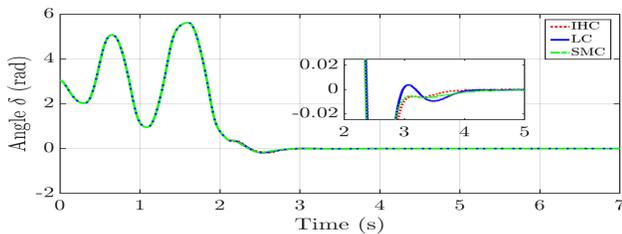
(b) Performance of rotary pendulum (α)

Fig. 3. Comparison of the performance in the IP stabilization

Euclidean norm of q. The IHC presents a better performance than the LC and SMC measured in terms of the closeness to the origin of the calculated norm. This fact is evident in Figure 4, where one may notice that the Euclidean norm of q converges faster and closer to zero in the IHC case (less than 4 s). Figure 5 shows the control signal provided to the rotary arm with the LC and IHC. *All experiments show better performance (faster convergence, higher precision, less control energy) of IHC* in comparison with the LC supported by the manufacturer. This is a consequence of the state dependent gain that characterizes the IHC resolution. Notice that this kind of adaptive gain represents a significant characteristic of
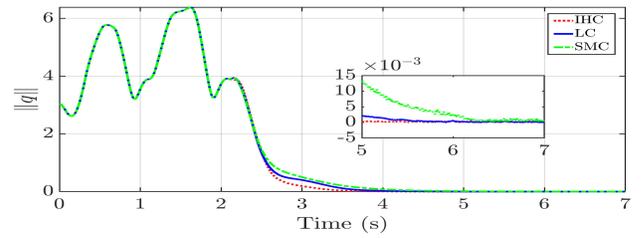

Fig. 4. Euclidean norm of the q without artificial perturbations
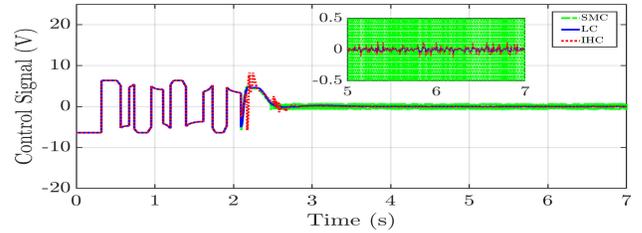
homogeneous controllers.

Fig. 5. Control signal of rotary arm.

With the aim of evidencing the steady-state performance of the proposed controller, the least mean square error (LMSE) of the stabilization error obtained with the IHC, LC, and SMC has been summarized in Table I.

This table compares the LMSE obtained with all the tested controllers without adding an artificial perturbation.

TABLE I
COMPARISON OF THE LMSE VALUE WITHOUT ARTIFICIAL
PERTURBATION.

Control	IHC	LC	SMC
LMSE	11.06	11.23	11.43

Notice that the implementation of the IHC offers from 1.5% to 3.23% improvement compared with the results obtained from the LC and the SMC implementation, respectively. In addition, notice that the improvement requires only 1.48% more energy compared with the consumed by the LC and 17.9% less than the SMC.

To verify the robustness of the proposed controller three additional experiments were made. This set of experiments considers a class of matched perturbation acting over the experimental setup. For this case, the matched perturbation was induced artificially in the Simulink-Matlab® implementation of the tested controllers, which means that the perturbation was coupled to the control signal. Here, the external perturbation was proposed as $G(0.02\sin(10t) + 0.01\sin(3t))$ with $G = \{1, 60, 200\}$ denoting a multiplicative gain to represent three different scenarios of the external perturbation.

Figure 6 depicts the comparison of the norms obtained with the proposed controller (IHC), the LC, and a first-order SMC when the system is affected by the proposed external perturbation. Here, it should be pointed out that this set of experiments did not consider in explicit form the presence of the external perturbation to recompute the control gains. Therefore, the three tested controllers were adjusted with the same gains used in the first set of experiments.
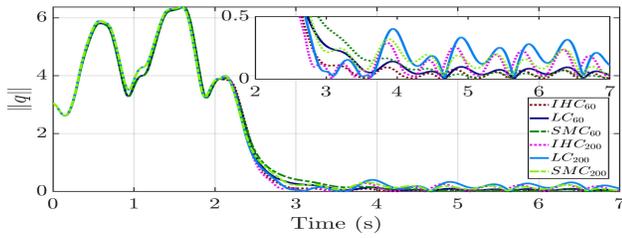
Fig. 6. Euclidean norm of q obtained with artificial perturbations.

TABLE II
COMPARISON OF THE LMSE VALUE WITH ARTIFICIAL PERTURBATION.

Control	IHC	LC	SMC
$LMSE_1$	11.08	11.26	11.47
$LMSE_{60}$	11.14	11.83	11.85
$LMSE_{200}$	11.47	12.14	12.13

The effectiveness of the proposed controller against external bounded perturbations has been demonstrated by the resulting performed states. Also, the faster convergence of the IHC in comparison with the LC and SMC is confirmed with the proposed comparative analysis (See Figure 6). Table II shows the obtained $LMSE$, the notation $LMSE_G$ with $G = \{1, 60, 200\}$ denotes the three scenarios under which the tests were done. From the results presented in Table II, it is clear that the IHC offers a significant improvement concerning the other tested controllers, but consuming similar energy that the LC.

VI. CONCLUSION

In this paper a scheme for inverse design of an IHC is proposed and a semi-explicit discretization scheme is developed to provide a well-posed digital implementation. Such approach allows us to update a (well-tuned) LC with a homogeneous nonlinear one, which guarantees a better performance (faster convergence, improved precision, lower control energy, etc.) of the control. The scheme is validated on real experiments with the IP. The comparison of the proposed controller to a LC and SMC confirms the superior transient response, smaller convergence region and controller with smaller amplitudes of the proposed controller implemented in a digital device.

REFERENCES

[1] Q. Sun, G. Yang, X. Wang, and Y. Chen, "Designing Robust Control for Mechanical Systems: Constraint Following and Multivariable Optimization," *IEEE Transactions on Industrial Informatics*, vol. 16, no. 8, pp. 5267–5275, 2020.

[2] R. Xu and Ü. Özgüner, "Sliding mode control of a class of underactuated systems," *Automatica*, vol. 44, no. 1, pp. 233–241, 2008.

[3] V. I. Utkin, *Sliding Modes in Control and Optimization*. Springer-Verlag, 1992.

[4] A. Levant, "Homogeneity approach to high-order sliding mode design," *Automatica*, vol. 41, no. 5, pp. 823–830, 2005.

[5] I. Boiko, L. Fridman, A. Pisano, and E. Usai, "Analysis of chattering in systems with second-order sliding modes," *IEEE Transactions on Automatic Control*, vol. 52, no. 11, pp. 2085–2102, 2007.

[6] A. Levant, "Chattering analysis," *IEEE Transactions on Automatic Control*, vol. 55, no. 6, pp. 1380–1389, 2010.

[7] A. Polyakov, D. Efimov, and W. Perruquetti, "Finite-time and fixed-time stabilization: Implicit Lyapunov function approach," *Automatica*, vol. 51, pp. 332–340, 2015.

[8] V. Utkin, "Discussion aspects of high-order sliding mode control," *IEEE Transactions on Automatic Control*, vol. 61, no. 3, pp. 829–833, 2016.

[9] A. Polyakov, "Sliding mode control design using canonical homogeneous norm," *International Journal of Robust and Nonlinear Control*, 2018.

[10] V. Acary and B. Brogliato, "Implicit Euler numerical scheme and chattering-free implementation of sliding mode systems," *Systems & Control Letters*, vol. 59, no. 5, pp. 284–293, 2010.

[11] O. Huber, V. Acary, B. Brogliato, and F. Plestan, "Implicit discrete-time twisting controller without numerical chattering: Analysis and experimental results," *Control Engineering Practice*, vol. 46, pp. 129–141, 2016.

[12] A. Polyakov, D. Efimov, and B. Brogliato, "Consistent Discretization of Finite-time and Fixed-time Stable Systems," *SIAM Journal on Control and Optimization*, vol. 57, no. 1, pp. 78–103, 2019.

[13] K. Zimenko, A. Polyakov, D. Efimov, and W. Perruquetti, "Generalized Feedback Homogenization and Stabilization of Linear MIMO Systems," in *Proc. 17th European Control Conference (ECC)*, 2018.

[14] V. I. Korobov, "A general approach to the solution of the problem of synthesizing bounded controls in a control problem," *Math. USSR SB*, vol. 37, pp. 535–539, 1979.

[15] J. Adamy and A. Flemming, "Soft variable-structure controls: a survey," *Automatica*, vol. 40, no. 11, pp. 1821–1844, 2004.

[16] H.-M. Joe and J.-H. Oh, "Balance recovery through model predictive control based on capture point dynamics for biped walking robot," *Robotics and Autonomous Systems*, vol. 105, pp. 1–10, 2018.

[17] S. Haddout, "Nonlinear reduced dynamics modelling and simulation of two-wheeled self-balancing mobile robot: Segway system," *Systems Science & Control Engineering*, vol. 6, no. 1, pp. 1–11, 2018.

[18] G. P. Neves, B. A. Angélico, and C. M. Agulhari, "Robust H2 controller with parametric uncertainties applied to a reaction wheel unicycle," *International Journal of Control*, vol. 93, no. 10, pp. 2431–2441, 2020.

[19] M. F. Hamza, H. J. Yap, I. A. Choudhury, A. I. Isa, A. Y. Zimit, and T. Kumbasar, "Current development on using rotary inverted pendulum as a benchmark for testing linear and nonlinear control algorithms," *Mechanical Systems and Signal Processing*, vol. 116, pp. 347–369, 2019.

[20] J. Moreno-Valenzuela, C. Aguilar-Avelar, S. A. Puga-Guzmán, and V. Santibáñez, "Adaptive neural network control for the trajectory tracking of the furuta pendulum," *IEEE Transactions on Cybernetics*, vol. 46, no. 12, pp. 3439–3452, 2016.

[21] J. Huang, M. Zhang, S. Ri, C. Xiong, Z. Li, and Y. Kang, "High-order disturbance-observer-based sliding mode control for mobile wheeled inverted pendulum systems," *IEEE Transactions on Industrial Electronics*, vol. 67, no. 3, pp. 2030–2041, 2019.

[22] R. Lozano, I. Fantoni, and D. J. Block, "Stabilization of the inverted pendulum around its homoclinic orbit," *Systems & Control Letters*, vol. 40, no. 3, pp. 197–204, 2000.

[23] X. Yang and X. Zheng, "Swing-up and stabilization control design for an underactuated rotary inverted pendulum system: Theory and experiments," *IEEE Transactions on Industrial Electronics*, vol. 65, no. 9, pp. 7229–7238, 2018.

[24] A. Polyakov, J.-M. Coron, and L. Rosier, "On Homogeneous Finite-Time Control for Linear Evolution Equation in Hilbert Space," *IEEE Transactions on Automatic Control*, 2018.

[25] H. K. Khalil, "Nonlinear systems," *Upper Saddle River*, 2002.

[26] M. W. Spong, S. Hutchinson, and M. Vidyasagar, *Robot modeling and control*. John Wiley & Sons, 2020.

[27] H. Hermes, "Homogeneous coordinates and continuous asymptotically stabilizing feedback controls," *Differential Equations, Stability and Control*, vol. 109, no. 1, pp. 249–260, 1991.

[28] A. Bacciotti and L. Rosier, *Liapunov functions and stability in control theory*. Springer Science & Business Media, 2006.

[29] S. N. Elaydi, *Differential equations: stability and control*. CRC Press, 1990.

[30] M. Vukobratovic, *Dynamics and robust control of robot-environment interaction*, vol. 2. World Scientific, 2009.

[31] D. T. Greenwood, *Principles of Dynamics*. Prentice-Hall Englewood Cliffs, NJ, 1988.

[32] J. Apkarian, M. Levis, and P. Martin, *Student Workbook QUBE-Servo 2 Experiment for Matlab/ Simulink Users*, Quanser, 2016.

[33] A. Polyakov, D. Efimov, and W. Perruquetti, "Robust stabilization of MIMO systems in finite/fixed time," *International Journal of Robust and Nonlinear Control*, vol. 26, no. 1, pp. 69–90, 2016.

[34] J.-P. Barbot, A. Levant, M. Livne, and D. Lunz, "Discrete differentiators based on sliding modes," *Automatica*, vol. 112, p. 108633, 2020.

[35] R. L. Burden and J. D. Faires, *Numerical Analysis*, 9th ed., M. Julet, Ed. Brooks Cole, 2010.

David Cruz-Ortiz received the M. Sc. degree in advanced technologies from UPIITA-IPN (Mexico) in 2015 and the Ph.D. degree in control sciences from the Department of Automatic Control, CINVESTAV-IPN (Mexico) in February 2020. From September 2018 to May 2019 he realized an internship research at Inria (Lille - Nord Europe Center). He is currently with the bio-engineering department at the Interdisciplinary School of Biotechnology, National Polytechnic Institute. His research interests include robust control, sliding modes, biomedical instrumentation, rehabilitation devices and robotic systems.

Mariana Ballesteros received the M.Sc. degree in advanced technologies from UPIITA-IPN in 2015 and the Ph.D. degree in control sciences from the Department of Automatic Control, CINVESTAV-IPN, February 2020. She is currently with the bio-engineering department at the Interdisciplinary School of Biotechnology, National Polytechnic Institute and with the Biomechatronics laboratory at the Tecnologico de Monterrey, School of Engineering and Sciences. Her research interests include artificial neural networks, robotics, adaptive programming, and robust control.

Andrey Polyakov received Ph.D. in Systems Analysis and Control from Voronezh State University in 2005. From 2004 up to 2010 he was a lecturer and, next, an associate professor with this university. In 2007 and 2008, he was working for the CINVESTAV-IPN center in Mexico City. From 2010 up to 2013 he was leader researcher of the Institute of the Control Sciences, Russian Academy of Sciences. In 2013 he joined Inria in Lille, France. He is a co-author of more than 150 publications in control theory and applications (including the books "Attractive Ellipsoids in Robust Control", "Road Map for Sliding Mode Control Design", "Generalized Homogeneity in Systems and Control"). His research interests include different aspects of nonlinear control and estimation theory such as finite-time\fixed-time stability, generalized homogeneity, sliding modes and Lyapunov methods for both finite dimensional and infinite dimensional systems.

Denis Efimov received Ph.D. degree in Automatic Control from the Saint-Petersburg State Electrical Engineering University (Russia) in 2001, and Dr.Sc. degree in Automatic control in 2006 from the Institute for Problems of Mechanical Engineering RAS (Saint-Petersburg, Russia). From 2006 to 2011 he was working in the L2S CNRS (Supelec, France), the Montefiore Institute (University of Liege, Belgium) and IMS CNRS lab (University of Bordeaux, France). In 2011, he joined Inria (Lille - Nord Europe center). Starting from 2018 he is the scientific head of Valse team. He is a member of several IFAC TCs and a Senior Member of IEEE. He is an author of more than 130 journal papers. He is also serving as an Associate Editor for IEEE Transactions on Automatic Control, Automatica, IFAC Journal on Nonlinear Analysis: Hybrid Systems and Asian Journal of Control.

Isaac Chairez received the B.S. degree in biomedical engineering from the National Polytechnic Institute (IPN), Mexico City, in 2002, and the master and Ph.D. degrees in control sciences from the Department of Automatic Control, Center of Investigation and Advanced Researching, IPN, in 2004 and 2007, respectively. He is currently with the Professional Interdisciplinary Unit of Biotechnology, IPN and with the Tecnologico de Monterrey, School of Engineering and Science. His current research interests include neural networks, fuzzy control theory, nonlinear control, adaptive control, and game theory.

Alex S. Poznyak graduated from the Moscow Physical Technical Institute (MPhTI) in 1970. He earned his Ph.D. and Doctor Degrees from the Institute of Control Sciences of the Russian Academy of Sciences in 1978 and 1989, respectively. From 1973 up to 1993 he served this institute as a researcher and leading researcher, and in 1993 he accepted a post of full professor (3-E) at CINVESTAV of IPN in Mexico. He is a Regular Member of the Mexican Academy of Sciences and System of National Investigators. He is a Fellow of IMA (Institute of Mathematics and Its Applications, Essex, UK) and Associated Editor of the Oxford-IMA Journal on Mathematical Control and Information, as well as the Iberoamerican International Journal on "Computations and Systems". He was also an Associated Editor of CDC, ACC and Member of the Editorial Board of IEEE CSS.